ADVANCED OPTICAL MATERIALS
www.advopticalmat.de

Striking Change in Radiative Lifetime and Asymmetry Ratio with Temperature for the Double Perovskite $Cs_2NaEuCl_6$

Daiwen Xiao, Hei-Yui Kai, Guohua Jia, Ka-Leung Wong, and Peter A. Tanner**

The measurement of quantum yield (QY) is an important process for a phosphor. This is often accomplished by the comparison of the low-temperature lifetime with the room temperature (RT) lifetime. It is shown that this procedure provides a considerable underestimation of QY in certain cases. Additionally, the use of the europium ion as an indicator of changes in site symmetry with temperature has severe limitations. This work reveals that a decrease in measured lifetime with increasing temperature of a system cannot always be associated with a descent in site symmetry and may be due to increasing radiative rate.

1. Introduction

The rate of spontaneous emission from a given energy level, A (s^{-1}), can be described by the Fermi Golden Rule, which comprises the relevant electronic transition moment and the density of electromagnetic modes of the environment. The reciprocal of the spontaneous emission rate is termed the radiative lifetime of the state, τ_R (s). Radiative lifetimes can vary from nanoseconds for electric dipole (ED) allowed transitions to milliseconds for magnetic dipole (MD) allowed transitions. However, the luminescent state may also be depopulated by nonradiative processes so that the measured lifetime, τ, is smaller than τ_R. The quantum yield of emission (QY) is given by the ratio τ/τ_R.

D. Xiao, H.-Y. Kai, P. A. Tanner
Department of Chemistry
Hong Kong Baptist University
Waterloo Road, Kowloon Tong, Hong Kong SAR, P. R. China
E-mail: monkey.tanner@polyu.edu.hk

G. Jia
School of Molecular and Life Sciences
Curtin University
Kent Street, Bentley, WA 6102, Australia

K.-L. Wong
Department of Applied Biology and Chemical Technology
The Hong Kong Polytechnic University
Hung Hom, Kowloon, Hong Kong SAR, P. R. China
E-mail: klgwong@polyu.edu.hk

The ORCID identification number(s) for the author(s) of this article can be found under https://doi.org/10.1002/adom.202302261

DOI: 10.1002/adom.202302261

The emission of pristine or doped lead-free halide double perovskites, $Cs_2MM'Cl_6$, previously known as elpasolites, has attracted much attention recently,[1] due to their photonics applications such as solar cell absorbers,[2a] photodetectors, photocatalysts [2b] and light emitting diodes.[2c] Here, M is a monovalent cation such as Na or Ag, and M' is a trivalent cation, such as Sb,[1b] Bi, [1c,d] V,[1e] or Cr.[1f] The materials are nontoxic. The QY at RT of several double perovskite nanoparticle systems have been reported to be remarkably high: for example, $Cs_2Ag_{0.6}Na_{0.4}InCl_6{:}Bi^{3+}$ 86 ± 5%.[1a] This implies that the radiative lifetime is almost the same as the measured lifetime. The $Cs_2MM'Cl_6$ systems may also comprise M' = Ln^{3+}, a tripositive lanthanide ion.[3] Lanthanide elpasolites emit light over a wide range of wavelengths, from UV (Ce^{3+}, Gd^{3+}),[4a,b] visible (Eu^{3+}, Tb^{3+}, Ho^{3+}, Er^{3+}),[4c–f] near-infrared (Nd^{3+}, Yb^{3+}),[4g,h] and infrared (Er^{3+}, Tm^{3+}).[4i,j] We focus upon Ln^{3+} = Eu^{3+} in this paper.

We consider the red emission from $^5D_0$ (where the notation is in terms of the quantum numbers $^{2S+1}L_J$) of the $4f^6$ ion Eu^{3+} in the system $Cs_2NaEuCl_6$ which crystallizes in the space group $Fm\bar{3}m$ (No. 225, **Figure 1a**). Contrary to other rare earth systems where the lanthanide ion occupies several sites,[5] the Eu^{3+} ions occupy only one site at the center of an octahedron of chloride ions in $Cs_2NaEuCl_6$. The electronic ground state $^7F_0$ lies below the valence band (Figure 1b) and the relevant electronic energy levels are shown in Figure 1c. The representative lifetime of Eu^{3+} systems normally lies in the (sub)ms range with the radiative rate ≈500 s^{-1}; but the quantum yield can vary over orders of magnitude (**Table 1**) and is rather smaller than that reported for the doped $Cs_2AgInCl_6$ material above. The $Cs_2NaEuCl_6$ system is extraordinary because all of the pure electronic transitions are forbidden by the ED mechanism. The observed spectral bands are due to i) orbitally allowed magnetic dipole (MD) transitions. Since these are allowed, the intensity is not sensitive to the environment of the Eu^{3+} ion; ii) vibrational-electronic (vibronic) structure comprising, in emission, lower energy Stokes bands, and higher energy anti-Stokes bands. These bands are separated from the electronic origin (zero phonon line, ZPL) by a very similar energy and represent the modes of vibration, according to certain selection rules. The intensities of the corresponding Stokes and anti-Stokes bands are related by a temperature-dependent Boltzmann factor.

Cabral et al.[6a] have noted that the temperature quenching of a lanthanide ion emitting level can occur by three main mechanisms: multi-phonon relaxation, energy transfer to

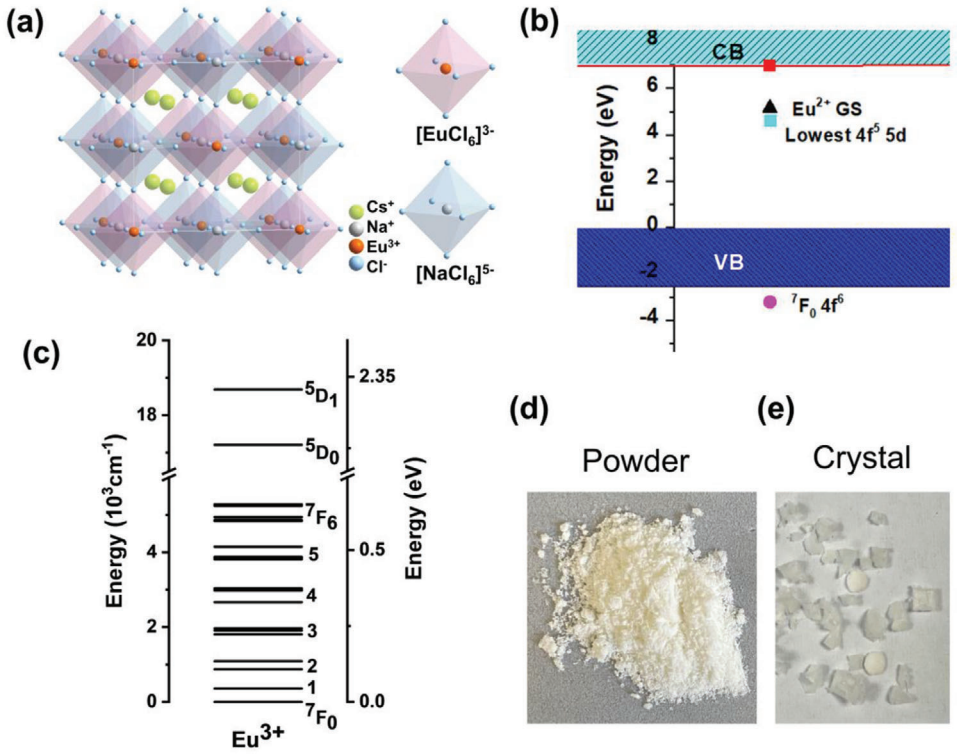

Figure 1. a) Crystal structure and b) Vacuum referred binding energy diagram of $Cs_2NaEuCl_6$. VB valence band, CB conduction band. c) Selected energy levels of Eu^{3+} showing $^5D_0$ emissive state and the large energy gap below it. Note the scale break. Photographs of d) powder (Method A) and e) crystal (Method B) samples of $Cs_2NaEuCl_6$.

ligand-localized electronic states (singlet or triplet) and the crossover from the 4f configuration to a charge-transfer (CT) state. For solid-state lanthanide systems, it has been usually assumed that the nonradiative rate of depopulation of a given level is very small at low temperatures, say ≤ 77 K. Hence the measured low-temperature lifetime has been equated with the radiative lifetime.[6b–e] The QY at RT then has been estimated by comparing the measured lifetime with this lifetime, as above, τ/τ_R. Herein, we show that the radiative rate may vary considerably with temperature in some cases so that such a comparison is not valid.

In fact, for the system under study, the radiative lifetime at low-temperature is almost double that at room temperature. The phenomenon of lifetime increase with temperature has recently been highlighted as negative-thermal quenching (NTQ).[7] The basic mechanism in the present case of radiative lifetime decrease with temperature is the relative increase in intensity of anti-Stokes vibronic structure with temperature.

The Eu^{3+} ion has often been employed as an indicator of site symmetry in materials. An increase in the ratio of emission intensity ratio of the transitions $(^5D_0 \rightarrow {}^7F_2)/(^5D_0 \rightarrow {}^7F_1)$ for Eu^{3+} (often called the asymmetry ratio, R2) is usually taken to indicate a descent in symmetry at the Eu^{3+} site. This may not be the case for systems where the observed transitions are not purely ED allowed, as herein.

Table 1. Representative $^5D_0$ emission lifetimes and quantum yields of Eu^{3+} systems.

	System	Phase	T [K]	τ [ms][a]	k_{rad}[s^{-1}][b]	%QY[c]	Ref.
1	$[EuGa_4(shi)_4(C_6H_5CO_2)_4(C_5H_5N)(CH_3OH)]$[d]	Solid	RT	0.242 (79%) 0.043 (21%)	-	0.016	[8]
2	[EuL]-[e]	Solution	RT	1.71	586	15.6	[9]
3	$C_4H_{11}Eu_2Na_4O_{16.5}P_4$	Rehydrated	RT	0.62	410[f]	25.4	[10]
4	$[Eu(tta)_3(pyphen)]$[g]	Solid	77	0.788	-	-	[6a]
		Solid	323	0.518	-	31.3	[6a]
5	$Eu(L2)_2$[h]	Solution	RT	0.234	573	5.1	[11]

[a] Measured lifetime; [b] Radiative rate; [c] Quantum yield; [d] Salicylhydroxamic acid (H_3shi); [e] 3,4,3-LI(1,2-HOPO); [f] There is a typo for the units in Ref.[10]; [g] {tris(thenoyltrifluoroacetone)pyrazino[2,3-f][1,10]phenanthroline}europium (III); [h] Refer to Ref.[11] for formula.

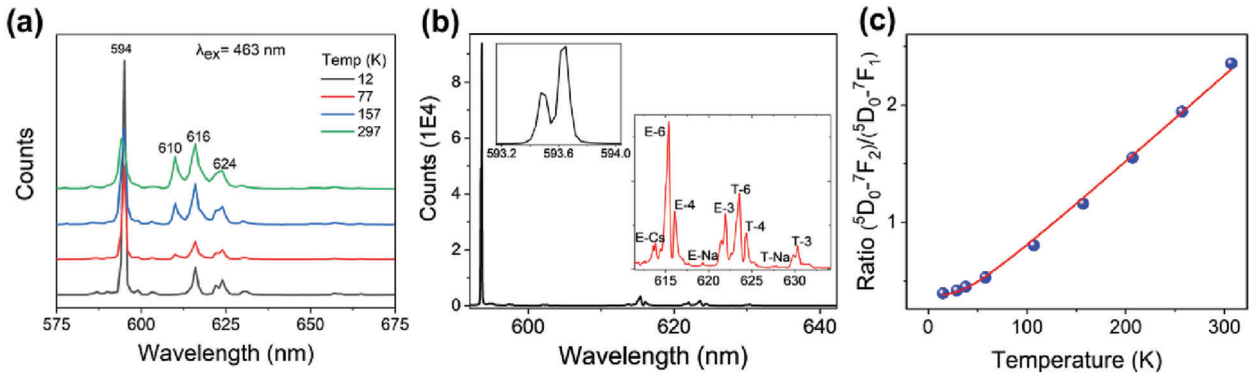

Figure 2. a) 463 nm Xe lamp excited emission spectrum of $Cs_2NaEuCl_6$ at different temperatures, recorded by the Fluorolog-3; b) 10 K Ar^+ 465 nm excited emission spectrum of $Cs_2NaEuCl_6$ recorded using an Acton 0.5 m monochromator. The first inset shows the $^5D_0 \rightarrow {}^7F_0$ zero phonon line on a finer scale. For the marked bands in the second inset, the luminescent state is $^5D_0$ and E, T correspond to the terminal electronic states $^7F_2$ (E_g, and T_{2g}) (O_h). The corresponding vibrations are marked in the expanded inset (corresponding to ν_1 (1)–ν_6 (6) moiety modes and consist of zone boundary, transverse and longitudinal optic components, TO and LO. Cs and Na correspond to unit cell group modes involving those ions. The components (in cm^{-1}) of the bending modes ν_6 and ν_4 are ≈66 (ZB), 77–80, and 98 (TO), 121 (LO), respectively; whereas the Cs^+ and Na^+ unit cell group modes are at 45, 56, and 176, respectively. c) Temperature dependence of the intensity ratio $(^5D_0 \rightarrow {}^7F_2)/(^5D_0 \rightarrow {}^7F_1)$. The experimental datapoints are fitted by Equation 1 with two free parameters A = 0.385±0.022 and $\hbar\omega$ = 72.0±4.4.

2. Results and Discussion

The compound $Cs_2NaEuCl_6$ was prepared by the evaporation method as a powder (Method A, Figure 1d) and by hydrothermal synthesis as crystals (Method B, Figure 1e) as described in the Supporting Information. The X-ray diffractogram of a sample prepared by Method A is shown in Figure S1 (Supporting Information). However, the luminescence spectrum is a much more sensitive test of the purity of a sample. The comparison with previous reports of the emission spectrum of $Cs_2NaEuCl_6$ shows that the spectra are the same.[5c,12a–c] We have measured the ratio of emission counts $(^5D_0 \rightarrow {}^7F_2)/(^5D_0 \rightarrow {}^7F_1)$, that is, R2, for this compound as a function of temperature from ≈12 K to RT. It is observed that the integrated counts of the $^5D_0 \rightarrow {}^7F_1$ transition (594 nm, **Figure 2a**) remain effectively constant since the bandwidth increases while the peak height decreases. This is normal for a MD allowed transition. However, the features in the $^5D_0 \rightarrow {}^7F_2$ region increase in intensity with temperature. These are ED allowed vibronic bands in nature and the increase in temperature is due to the appearance of anti-Stokes components, mainly associated with τ_{2u} Cl—Eu—Cl bend and (ν_6) and τ_{1u} Cl—Eu—Cl bend (ν_4) vibrations.[12d] Although there is a low-temperature phase transition for the early members of the $Cs_2NaLnCl_6$ series ($O_h \rightarrow C_{4h}$), the center of symmetry of Eu^{3+} remains. Figure 2b shows the 10 K spectrum under higher resolution. The 4 cm^{-1} splitting of the $^5D_0 \rightarrow {}^7F_1$ transition is resolved in the inset and the individual vibronic structure of terminal $^7F_2$ levels E_g and T_{2g} is labeled.

In summary, Figure 2a shows that the $^5D_0 \rightarrow {}^7F_2$ vibronic structure becomes stronger, relative to $^5D_0 \rightarrow {}^7F_1$, with increasing temperature. In the literature, changes in the R2 ratio are commonly associated with changes in the site symmetry of the Eu^{3+} ion. This is not so in the present case. The change is due to the hyperbolic cotangent dependence of the oscillator strength of a vibronic transition with temperature:[13]

$$Intensity Ratio\left\{\left[^5D_0 \rightarrow {}^7F_2\right] / \left[^5D_0 \rightarrow {}^7F_1\right]\right\} = \mathrm{Acoth}\left(\hbar\omega / (2kT)\right) \quad (1)$$

where A is a constant, $\hbar\omega$ is the vibration frequency, k is the Boltzmann constant and T is temperature. Figure 2b takes into account that most of the anti-Stokes vibronic intensity arises from the ν_6 mode and fits the temperature dependence of Equation 1. The fitted value of $\hbar\omega$ is 72 cm^{-1}, R_{adj}^2 = 0.9977.

2.1. $^5D_0$ Lifetime Temperature Dependence

The $^5D_0$ lifetime has been measured for samples of $Cs_2NaEuCl_6$ (coated in nujol oil for protection) prepared by the evaporation method A and the hydrothermal method B. **Figure 3a** shows the results for two different samples prepared by method A (labeled A1 and A2). The lifetimes are much longer than those previously reported for this system,[14a,b] which is attributed to the sample deliquescence.

We pause for a moment, to discuss the fitting of lifetime data in the time domain. This is for the general reader and is not essential to the paper. We do not find clarification or guidelines on this topic in the literature and hope to stimulate discussion and consensus from our observations. The aim is to show that different values can be obtained by using different fitting methods. We have only employed two methods herein. The fitting of the RT lifetime in each case was made over a certain timescale after the 460 nm Spectra LED pulse. We consider that a range of at least five lifetimes, leading to a count reduction ≥ 149, is necessary. Looking at the tail of the decay curve can enable measurement of the energy migration rate,[14a] but it may be difficult to differentiate from random noise. For weakly-emitting samples, it is common that the count rates at the start of measurement are distorted by stray light at wide slit widths. The exponential fits against time, t, using the three parameter (A, y_0, τ) equation:

$$\mathrm{Counts} = y_0 + \mathrm{Aexp}\left(-t/\tau\right) \quad (2)$$

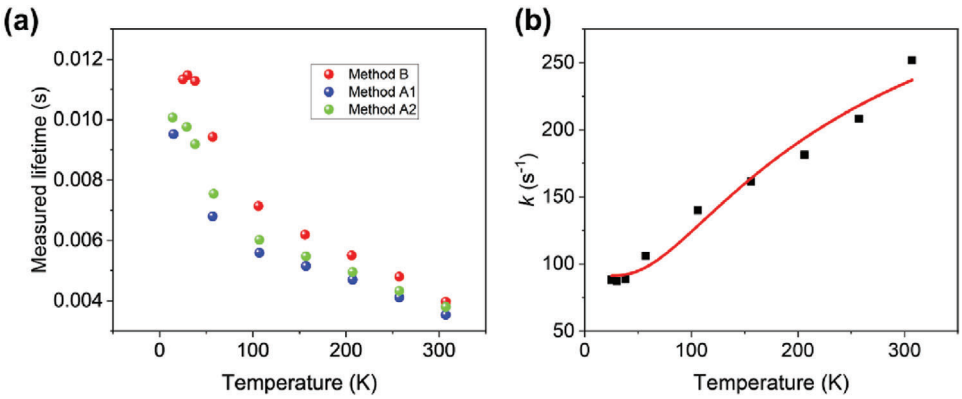

Figure 3. a) Variation of measured lifetime with temperature for different samples of $Cs_2NaEuCl_6$: A1, A2 prepared by evaporation method; B prepared by hydrothermal method. b) Measured reciprocal lifetime plotted against temperature for sample prepared by method B, fitted by Equation 6.

with, or without background subtraction, whereas the linear fits used the two-parameter (A, τ) equation:

$$\ln(\text{Counts}) = \ln A - t/\tau \tag{3}$$

The detailed comparison of fits using these equations is included in the Supporting Information. Taking natural logarithms compresses the data and minimizes the sum of squares error (SSE) for the transformed data, whereas the exponential fits minimize the SSE for the original data. Hence the measured lifetimes using linear fits tend to be slightly longer.

The measured decay curves at different temperatures for a sample prepared by Method B are presented in Figure S7 (Supporting Information). Figure 3a shows that the sample prepared by the hydrothermal method has longer lifetimes (decreasing from ≈11.4 ms at 25–30 K to 4.0 ms at 307 K) than samples prepared by the evaporation method. The former samples are more crystalline than the powder prepared by evaporation, and when coated by nujol the deliquescence is not as marked. The spontaneous emission rate (radiative rate) in s^{-1} for the channel $^5D_0 \rightarrow {}^7F_1$ is given by:[6e]

$$A_{MD}\left({}^5D_0 \rightarrow {}^7F_1\right) = 14.65n^3 \tag{4}$$

and since n, the refractive index (RI) of $Cs_2NaEuCl_6$ at 589 nm is 1.588 from interpolation of values from other $Cs_2NaLnCl_6$ members, $A_{MD} = 58.67\ s^{-1}$, giving the magnetic dipole radiative lifetime as 17.0 ms. The radiative lifetime of $^5D_0$ at low-temperature may be calculated by comparing the emission counts, $I_{0\text{-}J}$, of $^5D_0 \rightarrow {}^7F_J$, to that of $^5D_0 \rightarrow {}^7F_1$,[6e,15] or:

$$A({}^5D_0) = \frac{1}{\tau_R} = A_{MD}\left({}^5D_0 \rightarrow {}^7F_1\right)\sum_{J=0}^{6}\frac{I_{0-J}}{I_{0-1}} \tag{5}$$

which gives, from the 12 K spectrum in Figure 2a, $A(^5D_0) = 98.5\pm4.0\ s^{-1}$, leading to the radiative lifetime of 10.2±0.4 ms, without taking into account the temperature change of RI. Similarly, using Figure 2b, $A(^5D_0) = 90.4\ s^{-1}$, and the radiative lifetime is 11.1 ms. At any rate, comparison with the experimental lifetime >(11.4 ms) shows that the quantum yield at low-temperature is near unity.

Figure 2a shows that the ratio $I_{TOT}/I(^5D_0 \rightarrow {}^7F_1)$ at RT is much greater than at low-temperature, due to the temperature dependence of vibronic structure. In this case, the $^5D_0$ radiative lifetime at RT is calculated to be 5.9 ms. Hence, the enormous change in radiative lifetime is almost entirely due to the temperature dependence of vibronic structure. From the measured lifetime of 4 ms, the RT QY is predicted to be 68%. Our measurements using an integrating sphere (in the Supporting Information) using 527 nm excitation give the value of 59% with an error of 10%. The RT QY of the powder sample is rather less, at 41%, due to easier hydrolysis.

2.2. Quenching of $^5D_0$ Emission

Emission intensity may change with temperature due to a change in QY and/or a change in absorption strength, whereas the lifetime varies according to radiative and nonradiative rate changes. Since the highest energy phonon in $Cs_2NaEuCl_6$ is ν_1 (LO) ≈290 cm^{-1} and the energy gap $^5D_0 - {}^7F_6$ is 12 338 cm^{-1},[12d] the order of multiphonon decay from $^5D_0$ is 43 so that this process is slow. The $^5D_1$ Γ_4 level is at 1752 cm^{-1} above $^5D_0$ Γ_1 and back-transfer is negligible at the temperatures employed. The thermal quenching of lifetime may be due to the promotion of electrons over an energy gap ΔE to a trap state. This change in reciprocal lifetime ($1/\tau = k$) with temperature may be modeled by:

$$k = 1/\tau_R + A\exp(-\Delta E/0.695T) \tag{6}$$

as in Figure 3b. The derived parameters are $\tau_R = 11.0\pm0.7$ ms and $\Delta E = 153\pm29\ cm^{-1}$. The value of the radiative lifetime is in agreement with that calculated from the 12 K spectrum, Figure 2b. It is noted that we do not observe persistent luminescence from our sample after UV irradiation, on warming from 77 K to RT.

3. Conclusion

The low-temperature lifetime of an inorganic compound is often assumed to be equal to the radiative lifetime because the rate of nonradiative processes is slow at low-temperature. This radiative lifetime is then used together with the RT measured lifetime

to yield the QY. We have found that due to an increase in vibronic radiative rate, the radiative lifetime can decrease considerably with increasing temperature. Hence, there is a considerable underestimation of QY by taking the measured low-temperature lifetime. Our results can be generalized not only for lanthanide ions, but also for transition metal ions such as Mn^{4+} and Cr^{3+}, situated at octahedral, or other high symmetry sites. The QY is an important parameter for a phosphor and if one is equating the low-temperature lifetime to the radiative lifetime, there should be minimal spectral changes when warming from low-temperature to RT. This would not be the case for vibronic structures or hot band structures of forced electric dipole transitions. The increase in radiative rate with increasing temperature can be taken as an opposite example of NTQ. The mechanism herein differs from other reports. For a copper(I) iodide metal–organic layered framework, with increasing temperature, the ligand's electronic delocalization-to-localization transition occurs so that the temperature dependence of photoluminescence arises from the electronic localization to delocalization transition. Similarly, for other systems, the reasons for NTQ are different.[16]

The europium ion is often employed as a monitor of site symmetry in a crystal lattice. In particular, the intensity ratio, R2, of the transitions $(^5D_0 \rightarrow {}^7F_2)/(^5D_0 \rightarrow {}^7F_1)$ is employed as a standard in this respect. In the present case, the ratio R2 increases considerably with temperature whereas the symmetry point group of the Eu^{3+} ion actually increases from C_{4h} to O_h. We have herein identified one (of several other reasons) why R2 may not be a valid parameter to indicate symmetry descent. We anticipate this work will provide deep insight into the structure-property relationship of lanthanide ions or transition metal ions doped luminescent systems.

Supporting Information

Supporting Information is available from the Wiley Online Library or from the author.

Acknowledgements

G.J. acknowledges the financial support from the Australian Research Council (ARC) through Future Fellowship Scheme (FT210100509) and Discovery Project Scheme (DP220101959). K.-L.W. thanks the financial assistance from the Hong Kong Research Grants Council No. 12300021, NSFC/RGC Joint Research Scheme (N_HKBU209/21), and the Centre for Medical Engineering of Molecular and Biological Probes (AoE/M 401/20). The authors thank Menglin Song for recording the X-ray diffractogram, and Prof. Jianhua Hao for making his instrument available to them. The authors thank Dr. Waygen Thor for reading the manuscript and giving constructive comments.

Conflict of Interest

The authors declare no conflict of interest.

Data Availability Statement

The data that support the findings of this study are available in the supplementary material of this article.

Keywords

double perovskite, europium, negative thermal quenching, quantum yield, radiative lifetime

Received: September 14, 2023
Revised: October 20, 2023
Published online: November 23, 2023

[1] a) H. Tang, Y. Xu, X. Hu, Q. Hu, T. Chen, W. Jiang, L. Wang, W. Jiang, *Adv. Sci.* **2021**, *8*, 2004118; b) X. Li, D. Wang, Y. Zhong, F. Jiang, D. Zhao, S. Sun, P. Lu, M. Lu, Z. Wang, Z. Wu, Y. Gao, Y. Zhang, W. W. Yu, X. Bai, *Adv. Sci.* **2023**, *10*, 220757; c) A. Huang, M. Liu, C.-K. Duan, K.-L. Wong, P. A. Tanner, *Inorg. Chem. Front.* **2022**, *9*, 6379; d) H. Yang, X. Chen, Y. Chu, C. Sun, H. Lu, M. Yuan, Y. Zhang, G. Long, L. Zhang, X. Li, *Light Sci. Appl.* **2023**, *12*, 75; e) O. S. Wenger, H. U. Güdel, *Chem. Phys. Lett.* **2002**, *354*, 75; f) O. S. Wenger, R. Valiente, H. U. Güdel, *J. Chem. Phys.* **2001**, *115*, 3819.

[2] a) O. Stroyuk, O. Raievska, J. Hauch, C. J. Brabec, *Angew. Chem., Int. Ed.* **2023**, *62*, e202212668; b) L. Chu, W. Ahmad, W. Liu, J. Yang, R. Zhang, Y. Sun, J. Yang, X. Li, *Nano-Micro Lett.* **2019**, *11*, 16; c) S. Ghosh, H. Shankar, P. Kar, *Mater. Adv.* **2022**, *3*, 3742.

[3] P. Saghy, A. M. Brown, C. Chu, L. C. Dube, W. Zheng, J. R. Robinson, O. Chen, *Adv. Opt. Mater.* **2023**, 2300277.

[4] a) P. A. Tanner, C. S. K. Mak, N. M. Edelstein, K. M. Murdoch, G. Liu, J. Huang, L. Seijo, Z. Barandiarán, *J. Am. Chem. Soc.* **2003**, *125*, 13225; b) A. J. De Vries, G. Blasse, *J. Chem. Phys.* **1988**, *88*, 7312; c) O. A. Serra, L. C. Thompson, *Inorg. Chem.* **1976**, *15*, 504; d) R. W. Schwartz, H. G. Brittain, J. P. Riehl, W. Yeakel, F. S. Richardson, *Mol. Phys.* **1977**, *34*, 361; e) P. A. Tanner, *J. Chem. Soc., Faraday Trans. 2* **1987**, *83*, 1367; f) W. Ryba-Romanowski, G. Dominiak-Dzik, S. Golab, *J. Phys.: Condens. Matter.* **1994**, *6*, 1593; g) W. Stręk, Z. Mazurak, C. Szafranski, J. Hanuza, K. Hermanowicz, B. Jezowska-Trzebiatowska, *Chem. Phys.* **1984**, *84*, 269; h) P. A. Tanner, *Mol. Phys.* **1986**, *58*, 317; i) A. Huang, C.-K. Duan, K.-L. Wong, P. A. Tanner, *J. Mater. Chem. C* **2022**, *10*, 2950; j) P. A. Tanner, *Mol. Phys.* **1985**, *54*, 883.

[5] G. Morrison, A. M. Latshaw, N. R. Spagnuolo, H.-C. Zur Loye, *J. Am. Chem. Soc.* **2017**, *139*, 14743.

[6] a) F. M. Cabral, D. A. Gálico, I. O. Mazali, F. A. Sigoli, *Inorg. Chem. Commun.* **2018**, *98*, 29; b) M. T. Berry, P. S. May, H. Xu, *J. Phys. Chem.* **1996**, *100*, 9216; c) P. Froidevaux, J. C. G. Buenzli, *J. Phys. Chem.* **1994**, *98*, 532; d) Y. Liu, W. Luo, R. Li, G. Liu, M. R. Antonio, X. Chen, *J. Phys. Chem. C* **2008**, *112*, 686; e) M. H. V. Werts, R. T. F. Jukes, J. W. Verhoeven, *Phys. Chem. Chem. Phys.* **2002**, *4*, 1542.

[7] a) D. Zhang, J. Zhou, X. Cao, X. Ge, F. Tang, C. Zheng, J. Ning, S. Xu, *J. Phys. Chem. Lett.* **2023**, *14*, 6464; b) F. Tang, Z. Su, H. Ye, W. Gao, X. Pan, S. Xu, *ACS Omega* **2018**, *3*, 13704.

[8] C. Y. Chow, S. V. Eliseeva, E. R. Trivedi, T. N. Nguyen, J. W. Kampf, S. Petoud, V. L. Pecoraro, *J. Am. Chem. Soc.* **2016**, *138*, 5100.

[9] L. J. Daumann, D. S. Tatum, B. E. R. Snyder, C. Ni, G.-L. Law, E. I. Solomon, K. N. Raymond, *J. Am. Chem. Soc.* **2015**, *137*, 2816.

[10] F. N. Shi, L. Cunha-Silva, R. A. Sá Ferreira, L. Mafra, T. Trindade, L. D. Carlos, F. A. Almeida Paz, J. Rocha, *J. Am. Chem. Soc.* **2008**, *130*, 150.

[11] J. I. Pacold, D. S. Tatum, G. T. Seidler, K. N. Raymond, X. Zhang, A. B. Stickrath, D. R. Mortensen, *J. Am. Chem. Soc.* **2014**, *136*, 4186.

[12] a) A. F. Kirby, D. Foster, F. S. Richardson, *Chem. Phys. Lett.* **1983**, *95*, 507; b) J. P. Morley, T. R. Faulkner, F. S. Richardson, *J. Chem. Phys.* **1982**, *77*, 1710; c) C. D. Flint, F. L. Stewart-Darling, *Mol. Phys.* **1981**, *44*, 61; d) P. A. Tanner, Y.-L. Liu, *J. Alloys Compd.* **1994**, *204*, 93.

[13] M. Cieslak-Golonka, A. Bartecki, S. P. Sinha, *Coord. Chem. Rev.* **1980**, *31*, 251.
[14] a) M. Bettinelli, C. D. Flint, *J. Phys.: Condens. Matter* **1991**, *3*, 7053; b) M. R. Duckett, C. D. Flint, *SPIE* **1997**, *3176*, 108.
[15] K. Binnemans, *Coord. Chem. Rev.* **2015**, *295*, 1.
[16] a) X. Chen, X. Wu, L. Yue, L. Zhu, W. Pan, Z. Qi, S. Wang, J. Shao, *Appl. Phys. Lett.* **2017**, *110*, 5; b) F. Jahanbazi, Y. Mao, *Chem. Mater.* **2022**, *34*, 10538; c) C. Wang, Y. Cai, H. Zhang, Z. Liu, H. Lv, X. Zhu, Y. Liu, C. Wang, J. Qiu, X. Yu, X. Xu, *Inorg. Chem.* **2021**, *60*, 19365.